Journal of Natural and Artificial Scientific Systems, 2026, 3(3): 256-279

Electrochemical Removal of Lead (Pb^{2+}) from Aqueous Solutions Using Coal-Derived Carbon Quantum Dot-Modified Electrodes

Blessing Udofia Ebong

Received: 12 March 2026/Accepted: 18 July 2026/Published: 28 July 2026

Abstract: *Lead contamination of water resources poses significant environmental and public health challenges due to its toxicity, persistence, and bioaccumulative nature. This study investigated the electrochemical removal of lead ions (Pb^{2+}) from aqueous solutions using carbon quantum dot (CQD)-modified electrodes synthesized from unutilized low-grade lignite coal. The CQDs, previously synthesized and characterized by Eddy et al. (2026a), were employed as active electrode materials owing to their high surface area, abundant oxygen-containing functional groups, and favorable electron transfer properties. Batch electrochemical experiments were conducted to evaluate the effects of initial Pb^{2+} concentration (10–200 mg L^{-1}), solution pH (2–8), applied potential (0.5–2.5 V), electrolysis time (10–180 min), and supporting electrolyte concentration (0.01–0.50 M Na_2SO_4) on lead removal efficiency. The results revealed that Pb^{2+} removal efficiency decreased slightly from 95.80% to 87.59% as the initial lead concentration increased from 10 to 200 mg L^{-1}, while the adsorption capacity increased from 23.95 to 437.93 mg g^{-1}. The removal efficiency improved significantly with increasing pH, reaching a maximum value of 94.66% at pH 8. Similarly, increasing the applied potential enhanced Pb^{2+} removal from 71.36% at 0.5 V to 96.55% at 2.5 V. Electrolysis time strongly influenced the process, with removal efficiency increasing from 37.55% after 10 min to 96.98% after 180 min. The presence of supporting electrolyte improved solution conductivity and charge transfer, resulting in an increase in removal efficiency from 84.52% at 0.01 M Na_2SO_4 to 96.85% at 0.50 M Na_2SO_4. Under the optimum operating conditions of pH 7.0, applied potential of 2.0 V, electrolysis time of 120 min, initial Pb^{2+} concentration of 100 mg L^{-1}, and 0.10 M Na_2SO_4, the CQD electrode achieved a removal efficiency of 96.08% with an adsorption capacity of 240.20 mg g^{-1}.Kinetic studies demonstrated that the adsorption process was best described by the pseudo-second-order model (R^2=0.9977), compared to the pseudo-first-order model (R^2=0.942 0.94), indicating that chemisorption was the dominant mechanism controlling Pb^{2+} uptake. The intraparticle diffusion model exhibited a lower correlation coefficient (R^2=0.889) and a significant intercept, confirming that diffusion was not the sole rate-controlling step. The overall removal mechanism involved surface complexation of Pb^{2+} ions with oxygen-containing functional groups followed by electrochemical reduction and deposition on the electrode surface. The study demonstrates that lignite coal-derived carbon quantum dots are highly effective electrode materials for the electrochemical remediation of lead-contaminated water. Their high removal efficiency, substantial adsorption capacity, and favorable kinetic behavior highlight their potential as sustainable, low-cost, and environmentally friendly materials for wastewater treatment applications.*

Keywords*: Carbon quantum dots; Lead removal; Electrochemical treatment; Heavy metal remediation; Adsorption kinetics; Lignite coal; Wastewater treatment.*

Blessing Udofia Ebong
Western Illinois University, USA, Department of Chemistry
Email: bu-ebong@wiu.edu
https://orcid.org/0009-0001-5254-2050

NASS

1.0 Introduction

Lead (Pb^{2+}) contamination of water resources has emerged as one of the most pressing environmental and public health challenges worldwide due to rapid industrialization, urbanization, mining activities, battery manufacturing, metal plating, pigment production, and improper waste disposal practices. (Akpakpan *et al*., 2024; Eddy *et al*., 2024). Lead is a non-essential and highly toxic heavy metal that persists in the environment because it is non-biodegradable and can accumulate in living organisms through the food chain (Ogburu *et al*., 2024; Udo *et al*., 2018). Its widespread industrial use, affordability, and accessibility have contributed significantly to increasing environmental concentrations of lead, particularly in developing countries where environmental monitoring and wastewater treatment infrastructure remain inadequate. Exposure to lead-contaminated water poses severe health risks, including neurological disorders, renal dysfunction, cardiovascular diseases, reproductive abnormalities, hematological disorders, and developmental impairments in children. Furthermore, lead exhibits a strong tendency to bioaccumulate in bones and soft tissues, where it can remain for decades and continue exerting toxic effects even after exposure has ceased.

Recent studies have highlighted the global burden of lead exposure and its associated health consequences. Rawat & Singh (2026) reported that lead toxicity affects multiple organ systems, including the respiratory, nervous, cardiovascular, hepatic, renal, skeletal, and reproductive systems, while also exhibiting genotoxic and carcinogenic effects. Similarly, Flora *et al*. (2012) observed that lead-induced oxidative stress contributes significantly to cellular damage and disease manifestation. Karokatose & Adewumi (2026) further emphasized that vulnerable populations, especially children and pregnant women, are at greater risk because lead can cross the placental barrier and interfere with fetal development. Bereda (2026) estimated that approximately 800 million children worldwide have blood lead levels exceeding recommended limits, underscoring the urgent need for effective remediation technologies.

Various treatment technologies have been developed for the removal of lead ions from aqueous solutions, including chemical precipitation, ion exchange, membrane filtration, coagulation-flocculation, adsorption, and electrochemical methods. Among these techniques, adsorption has attracted considerable attention due to its simplicity and high removal efficiency. Several adsorbents have been investigated, including Mg-Al layered double hydroxide/EDTA-coated zeolites, magnetic chitosan nanocomposites, agricultural biomass residues, and natural plant-derived materials. Sayyad *et al*. (2026) reported complete (100%) removal of Pb^{2+} using a Mg-Al layered double hydroxide/EDTA-zeolite nanocomposite under optimized conditions. Likewise, Abo Markeb *et al*. (2023) achieved 98.1% lead removal using a magnetic chitosan-cellulose nanocomposite with an adsorption capacity of 555.56 mg g^{-1}. Sustainable biomass-based adsorbents have also demonstrated promising lead sequestration performance in wastewater treatment applications (Akpanudo *et al*., 2024, 2026a)

Despite the effectiveness of adsorption techniques, challenges such as adsorbent regeneration, secondary waste generation, limited selectivity, and reduced efficiency in complex water matrices have stimulated interest in alternative treatment approaches (Ebong, 2025). Electrochemical technologies have emerged as promising alternatives because they combine high removal efficiency, operational simplicity, environmental friendliness, and the potential for metal recovery. Electrochemical removal typically

involves the reduction and deposition of dissolved metal ions onto the electrode surface, thereby minimizing secondary pollution. Liu *et al*. (2013) demonstrated lead removal efficiencies ranging from 97.2% to 99.6% using stainless steel net electrodes coated with single-walled carbon nanotubes, indicating the significant role of nanostructured electrode materials in enhancing electrochemical performance. More recently, Wu *et al*. (2026) developed a covalent organic framework-hollow mesoporous carbon sphere composite electrode that achieved 96% Pb^{2+} removal with remarkable selectivity in multicomponent water systems, highlighting the importance of advanced electrode architectures in electrochemical remediation.

Graphene oxide (GO) has attracted considerable attention as an electrode material because of its exceptional surface area, excellent mechanical strength, abundant oxygen-containing functional groups, and high adsorption capacity for heavy metal ions. The presence of hydroxyl, epoxy, and carboxyl groups on graphene oxide facilitates strong interactions with Pb^{2+} ions through electrostatic attraction and surface complexation mechanisms. However, the relatively low electrical conductivity of graphene oxide may limit its electrochemical performance. To overcome this limitation, carbon quantum dots (CQDs) have recently emerged as attractive nanomaterials for electrode modification. Carbon quantum dots possess unique physicochemical properties, including high surface area, tunable electronic characteristics, excellent conductivity, low toxicity, chemical stability, and abundant surface functional groups capable of binding heavy metal ions. The incorporation of CQDs into graphene oxide matrices can improve charge transfer, increase active sites, enhance electron mobility, and promote electrocatalytic activity, thereby improving the overall efficiency of electrochemical lead removal.

Although significant progress has been made in the development of nanostructured electrodes for heavy metal remediation, the application of carbon quantum dot/graphene oxide composite electrodes for the electrochemical removal of Pb^{2+} from aqueous solutions remains insufficiently explored. Most previous studies have focused on adsorption-based removal techniques or electrochemical systems employing carbon nanotubes, mesoporous carbons, or covalent organic framework composites. Limited information exists regarding the synergistic effects of CQDs and graphene oxide on lead ion adsorption, electron transfer kinetics, electrochemical deposition behavior, removal efficiency, and electrode stability. Furthermore, comprehensive studies integrating electrochemical characterization techniques such as cyclic voltammetry (CV), electrochemical impedance spectroscopy (EIS), and removal kinetics are scarce (Eddy *et al*., 2026b, c).

Therefore, this study aims to develop and evaluate carbon quantum dot/graphene oxide (CQD/GO) composite electrodes for the electrochemical removal of Pb^{2+} ions from aqueous solutions. Specifically, the study seeks to synthesize and characterize the CQD/GO electrodes, investigate the effects of operational parameters on lead removal efficiency, evaluate electrochemical behavior using advanced characterization techniques, and determine the mechanisms responsible for Pb^{2+} removal.

The significance of this study lies in its potential to contribute to the development of efficient, sustainable, and environmentally friendly technologies for heavy metal remediation. The integration of carbon quantum dots with graphene oxide is expected to enhance electrode conductivity, increase active adsorption sites, improve electrochemical reduction processes, and facilitate electrode regeneration. The findings will provide valuable insights into the design of

advanced nanostructured electrodes for wastewater treatment and may support the development of scalable electrochemical systems capable of addressing lead contamination in industrial effluents and drinking water supplies. Ultimately, the study aligns with global efforts to ensure safe water resources, protect public health, and achieve sustainable environmental management.

2.0 Materials and Method

3.1 Materials

All chemicals and reagents used in this study were of analytical grade and were used without further purification. Lead nitrate [$Pb(NO_3)_2$] was employed as the source of lead ions for the preparation of synthetic wastewater. Sodium sulfate (Na_2SO_4) was used as the supporting electrolyte during the electrochemical experiments, while hydrochloric acid (HCl) and sodium hydroxide (NaOH) were utilized for pH adjustment. Deionized water was used throughout the study for solution preparation, washing, and dilution purposes. Carbon quantum dots (CQDs) synthesized from low-grade lignite coal according to the method reported by Eddy *et al*. (2026a) served as the active nanomaterial for electrode fabrication.

The electrochemical experiments were conducted using a conventional three-electrode system connected to a computer-controlled potentiostat/galvanostat. The fabricated carbon quantum dot-modified electrode was used as the working electrode, a platinum wire served as the counter electrode, and an Ag/AgCl electrode functioned as the reference electrode. A glass electrochemical cell with a working volume of 250 mL was employed for all electrochemical studies.

Characterization of the synthesized carbon quantum dots and fabricated electrodes was carried out using several analytical instruments. Surface morphology and elemental composition were examined using Scanning Electron Microscopy coupled with Energy Dispersive X-ray Spectroscopy (SEM-EDS). Structural properties were investigated using X-ray Diffraction (XRD), while surface functional groups were identified using Fourier Transform Infrared Spectroscopy (FTIR). Raman spectroscopy was employed to assess the degree of graphitization and structural defects in the carbon materials. Ultraviolet-Visible (UV-Vis) spectroscopy was used to evaluate the optical properties of the synthesized CQDs.

The concentration of residual lead ions before and after electrochemical treatment was determined using an Atomic Absorption Spectrophotometer (AAS). Other laboratory equipment used during the study included an analytical balance, magnetic stirrer with heating facility, ultrasonic bath, centrifuge, vacuum filtration unit, laboratory oven, pH meter, and micropipettes for accurate measurement and preparation of solutions.

3.2 Synthesis of Carbon Quantum Dots (CQDs)

Carbon quantum dots (CQDs) used for the fabrication of the electrochemical electrode were synthesized according to the method reported by Eddy *et al*. (2026a) with slight modifications. Lignite coal obtained from an abandoned coal mine in Enugu State, Nigeria, was used as the carbon precursor. Prior to synthesis, the coal was purified to remove ash, mineral matter, and metallic impurities that could interfere with the oxidation process and adversely affect the quality of the resulting nanomaterial.

The raw coal sample was first dried in a laboratory oven at 105 °C for 24 h to eliminate moisture. The dried coal was subsequently pulverized using a planetary ball mill (Retsch PM100) operated at 400 rpm for 2 h to obtain a fine powder with enhanced surface area and improved reactivity. Approximately 5.0 g of the pulverized coal was transferred into a 250 mL round-bottom reflux flask containing 60 mL of an oxidizing acid mixture consisting of

concentrated nitric acid (HNO_3, 65%) and concentrated sulfuric acid (H_2SO_4, 98%) in a volume ratio of 3:1.

The reaction mixture was heated under reflux at 120 °C for 4 h with continuous magnetic stirring. During this oxidation process, the aromatic carbon framework of the lignite coal underwent oxidative fragmentation and surface functionalization, leading to the formation of nanosized carbon quantum dots enriched with oxygen-containing functional groups. After completion of the reaction, the mixture was allowed to cool naturally to room temperature.

The resulting suspension was filtered to remove unreacted carbonaceous residues and larger particles. The filtrate containing the CQDs was repeatedly washed with deionized water until near-neutral pH was attained. The purified CQD suspension was then centrifuged at 10,000 rpm for 20 min to further remove residual impurities and large aggregates. The supernatant containing dispersed carbon quantum dots was collected and stored at 4 °C for subsequent electrode fabrication.

The synthesized CQDs were characterized using Fourier Transform Infrared Spectroscopy (FTIR), Ultraviolet–Visible Spectroscopy (UV–Vis), X-ray Diffraction (XRD), Raman Spectroscopy, Scanning Electron Microscopy coupled with Energy Dispersive X-ray Spectroscopy (SEM–EDS), X-ray Photoelectron Spectroscopy (XPS), and nitrogen adsorption-desorption analysis to determine their structural, morphological, elemental, optical, and surface properties. Eddy *et al*. (2026) reported that the synthesized CQDs consisted of more than 90% carbon with sulfur, nitrogen, oxygen, and silicon heteroatom dopants, possessed predominantly amorphous structures, exhibited band gap energies of 2.61–2.68 eV, and showed a surface area of approximately 52 $m^2\ g^{-1}$, making them suitable candidates for electrochemical applications and heavy metal ion remediation.

3.3 Fabrication of Carbon Quantum Dot Electrode

The carbon quantum dots (CQDs) synthesized from low-grade lignite coal by Eddy *et al*. (2026) were utilized as the active electrode material in this study. Prior to electrode fabrication, the synthesized CQDs were dispersed in deionized water and ultrasonicated for 30 min to obtain a homogeneous suspension. A measured quantity of the CQD suspension was mixed with a small amount of Nafion solution, which served as a binder to enhance adhesion of the nanomaterial to the electrode surface. The resulting slurry was uniformly deposited onto the surface of a pre-cleaned glassy carbon electrode using the drop-casting technique. The modified electrode was subsequently dried in an oven at 60 °C for 12 h to ensure complete solvent evaporation and firm attachment of the CQD film. The prepared electrode was designated as CQD/GCE and stored in a desiccator until further use.

3.4 Preparation of Lead Solution

A stock solution containing 1000 mg L^{-1} Pb^{2+} was prepared by dissolving an accurately weighed amount of lead nitrate [$Pb(NO_3)_2$] in deionized water. Experimental solutions of varying concentrations (10, 20, 50, 100, 150, and 200 mg L^{-1}) were prepared by serial dilution of the stock solution. The pH of the solutions was adjusted using 0.1 M hydrochloric acid (HCl) or 0.1 M sodium hydroxide (NaOH) as required.

3.5 Electrochemical Removal of Pb^{2+} Ions

The electrochemical removal experiments were conducted in a conventional three-electrode electrochemical cell connected to a computer-controlled potentiostat/galvanostat. The CQD/GCE served as the working electrode, a platinum wire functioned as the counter electrode, and an Ag/AgCl electrode was used as the reference electrode. Sodium sulfate (0.1 M Na_2SO_4) was employed as the supporting electrolyte.

For each experiment, 250 mL of Pb^{2+} solution was transferred into the electrochemical reactor and continuously stirred at 300 rpm to ensure uniform mass transfer. Electrochemical treatment was carried out under different operating conditions to investigate the influence of process variables on lead removal efficiency. The parameters studied included initial Pb^{2+} concentration (10–200 mg L^{-1}), solution pH (2–8), applied potential (0.5–2.5 V), treatment time (10–180 min), and electrolyte concentration (0.01–0.50 M). Samples were collected at predetermined intervals and filtered prior to analysis.

3.6 Determination of Lead Removal Efficiency

The concentration of Pb^{2+} ions before and after electrochemical treatment was determined using Atomic Absorption Spectrophotometry (AAS). The percentage removal efficiency was calculated using equation 1 (Eddy *et al*., 2023a,b)

$$Removal\ efficiency\ (\%) = \frac{C_0 - C_i}{C_0} \times \frac{100}{1} \quad (1)$$

where C_0 is the initial Pb^{2+} concentration (mg L^{-1}) and C_i is the concentration after electrochemical treatment (mg L^{-1}).

3.8 Adsorption Capacity of the Electrode

The adsorption capacity of the CQD electrode towards Pb^{2+} ions was determined according to equation 2

$$q_e = \frac{(C_0 - C_e)}{m} \quad (2)$$

where q_e is the adsorption capacity (mg g^{-1}), C_0 is the initial Pb^{2+} concentration (mg L^{-1}), C_e is the equilibrium concentration (mg L^{-1}), V is the volume of solution (L), and m is the mass of CQDs deposited on the electrode (g).

3.9 Kinetic Studies

The kinetics of lead removal were analyzed using pseudo-first-order (equation 3) and pseudo-second-order kinetic models (equation 4)(Kelle *et al*., 2023)

$$ln(q_e - q_t) = lnq_e - k_1 t \quad (3)$$

$$\frac{t}{q_t} = \frac{1}{k_2 q_t^2} + \frac{t}{q_e} \quad (4)$$

where q_t is the amount of Pb^{2+} removed at time t, q_e is the equilibrium adsorption capacity, k_1 is the pseudo-first-order rate constant, and k2k_2k2 is the pseudo-second-order rate constant.

3.10 Electrode Regeneration and Reusability

The reusability of the CQD electrode was evaluated through successive electrochemical treatment cycles. After each cycle, the electrode was immersed in 0.1 M HCl solution for 15 min to desorb deposited lead ions. The electrode was then rinsed thoroughly with deionized water and reused under identical operating conditions. The removal efficiency after each cycle was recorded to assess electrode stability and regeneration performance.

3.11 Statistical Analysis

All experiments were conducted in triplicate, and the results were expressed as mean ± standard deviation. Statistical analysis was performed using SPSS version 27. Analysis of variance (ANOVA) was employed to determine the significance of the effects of operating parameters on lead removal efficiency at a confidence level of 95% ($p < 0.05$). Graphical representations and kinetic model fitting were carried out using OriginPro 2025 software.

3.0 Results and Discussion

3.1 Physicochemical Characteristics of Carbon Quantum Dots

The carbon quantum dots (CQDs) employed in this study were synthesized and comprehensively characterized by Eddy *et al*. (2026). The characterization results revealed that the synthesized CQDs possessed physicochemical properties suitable for electrochemical applications, particularly in heavy metal remediation. The CQDs exhibited a high carbon content, abundant oxygen-containing surface functional groups, nanoscale particle dimensions, and excellent

surface characteristics capable of facilitating adsorption and electrochemical reduction of Pb^{2+} ions.

The elemental composition of the synthesized CQDs is presented in Table 1. Carbon was identified as the predominant constituent, accounting for over 90% of the total composition. Minor quantities of oxygen, sulfur, nitrogen, and silicon were also detected, indicating successful heteroatom doping during the synthesis process. The presence of these heteroatoms is advantageous because they introduce additional active sites for metal ion adsorption and enhance electron transfer during electrochemical reactions.

The high carbon content observed in the CQDs suggests the formation of a highly carbonized nanostructure capable of facilitating electrical conductivity and electron transport. The oxygen-containing groups present on the CQD surface provide coordination sites for Pb^{2+} ions through electrostatic attraction and complexation mechanisms. Similar observations have been reported for carbon-based nanomaterials used in electrochemical water treatment systems.

Table 1: Elemental Composition of Lignite Coal-Derived Carbon Quantum Dots (Eddy *et al*., 2026)

Element	Composition (%)
Carbon (C)	90.62
Oxygen (O)	5.84
Sulfur (S)	1.76
Nitrogen (N)	1.12
Silicon (Si)	0.66

(Source: Adapted from Eddy *et al*. (2026a)

The structural properties of the synthesized CQDs were evaluated using X-ray diffraction analysis. The XRD pattern showed a broad diffraction peak centered around $2\theta = 24°$, indicating the predominance of amorphous carbon structures with a low degree of graphitization. The absence of sharp crystalline peaks suggests successful conversion of lignite coal into nanoscale carbon particles.

The XRD of the CQDs was clearly described and presented in the work published by Eddy *et al*. (2026). The amorphous nature of the CQDs is beneficial for adsorption and electrochemical processes because disordered carbon structures generally possess a greater number of defects and active sites than highly crystalline materials. These defects can serve as nucleation sites for lead ion deposition during electrochemical treatment.

Fourier Transform Infrared Spectroscopy (FTIR) analysis revealed the presence of several oxygen-containing functional groups on the CQD surface. The major absorption bands observed were as shown in Table 2.

The FTIR results confirm the presence of hydroxyl, carbonyl, and carboxyl functional groups on the CQD surface. These groups play a critical role in the adsorption and electrochemical removal of Pb^{2+} ions by providing negatively charged sites that facilitate metal ion binding.

The optical properties of the synthesized CQDs were investigated using UV–Visible spectroscopy. The UV–Vis spectra exhibited characteristic absorption peaks associated with $\pi \rightarrow \pi^*$ and $n \rightarrow \pi^*$ electronic transitions, confirming the formation of nanosized carbon structures. The band gap energy was determined using the Tauc relationship (Eddy *et al*., 2026)

Table 2: Major FTIR Functional Groups Identified in the Synthesized CQDs

Wavenumber (cm^{-1})	Functional Group
3420	O–H Stretching
2920	C–H Stretching
1715	C=O Stretching
1620	C=C Aromatic Stretching
1380	C–N Stretching
1100	C–O Stretching

The calculated band gap energy ranged from 2.61 to 2.68 eV, indicating semiconducting behavior suitable for electrochemical applications. Other physicochemical properties reported for the CQDs are provided in Table 3

Table 3: Surface and Optical Characteristics of the Synthesized CQDs

Property	Value
Surface Area (m^2 g^{-1})	52.0
Average Particle Size (nm)	4.5–8.0
Pore Volume (cm^3 g^{-1})	0.143
Band Gap Energy (eV)	2.61–2.68
Structural Nature	Predominantly Amorphous

The relatively high surface area of 52 m^2 g^{-1} provides numerous active sites for Pb^{2+} adsorption and electrochemical deposition. Furthermore, the nanoscale dimensions of the CQDs facilitate rapid electron transport and improve the accessibility of adsorption sites. Fig. 1 illustrates the adsorption and electrochemical reduction of Pb^{2+} ions on oxygen-containing functional groups located on the CQD surface.

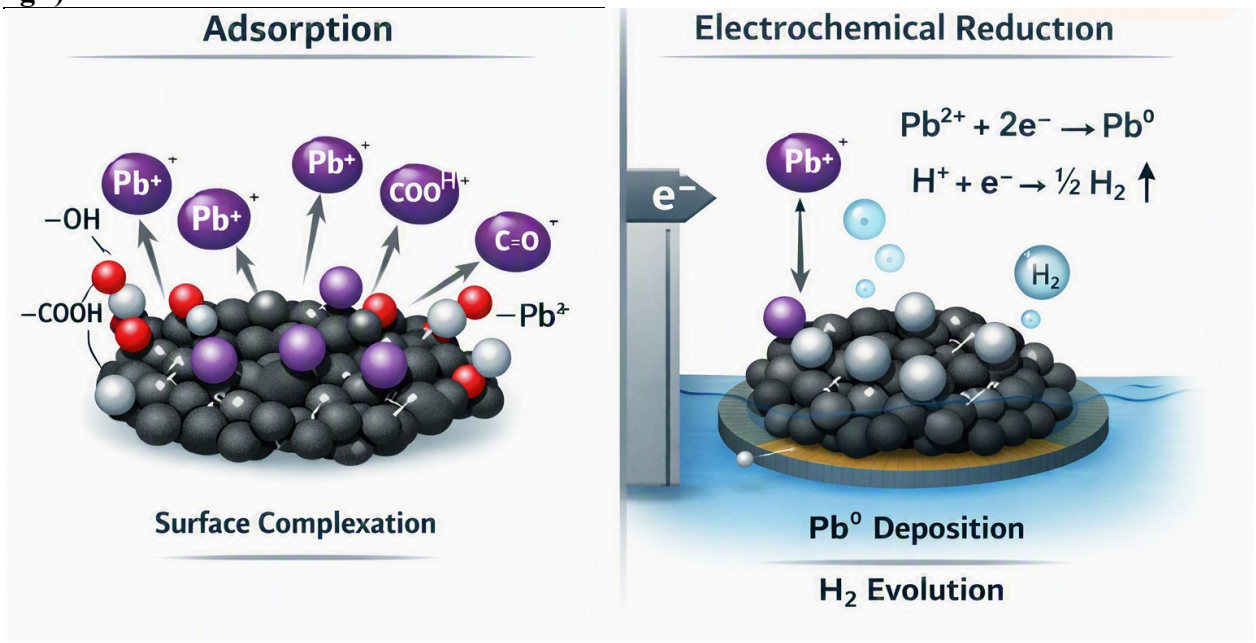

Fig. 2: Proposed Mechanism of Pb^{2+} Interaction with CQDs

The mechanism of Pb^{2+} removal by CQDs involves both adsorption and electrochemical reduction processes. Initially, Pb^{2+} ions migrate toward the negatively charged oxygen-containing functional groups present on the CQD surface. The interaction may be represented as:

$$CQD - COO^- + Pb^{2+} \rightarrow (CqD - COO)_2 Pb \quad (5)$$

Subsequently, under an applied electrical potential, the adsorbed Pb^{2+} ions undergo electrochemical reduction according to equation 6

$$Pb^{2+} + 2e^- \rightarrow Pb^0 \quad (6)$$

where metallic lead is deposited on the electrode surface. The physicochemical properties reported by Eddy *et al*. (2026) indicate that the lignite coal-derived CQDs possess the structural, optical, and surface characteristics required for efficient electrochemical remediation of lead-contaminated water. Their high carbon content, abundant functional groups, moderate surface

area, and semiconducting behavior make them promising electrode materials for Pb^{2+} removal applications.

4.2 Effect of Initial Pb^{2+} Concentration on Electrochemical Removal Efficiency

The initial concentration of Pb^{2+} ions is one of the most important factors influencing the performance of electrochemical treatment systems because it determines the driving force for mass transfer, electrode surface utilization, and availability of active adsorption sites. In the present study, the effect of initial lead concentration on the removal efficiency of the carbon quantum dot (CQD)-modified electrode was investigated over a concentration range of 10–200 mg L^{-1} under constant operating conditions of pH 6.0, applied potential of 1.5 V, treatment time of 120 min, and electrolyte concentration of 0.1 M Na_2SO_4. The experimental results are presented in Table 4.

The results show that the CQD electrode exhibited excellent lead removal performance across the investigated concentration range. The removal efficiency decreased slightly from 95.80% at 10 mg L^{-1} to 87.59% at 200 mg L^{-1}.

Table 4. Effect of Initial Pb^{2+} Concentration on Electrochemical Removal Efficiency

Initial Concentration (mg L^{-1})	Final Concentration (mg L^{-1})	Removal Efficiency (%)	Adsorption Capacity, qe (mg g^{-1})
10	0.423	95.79	23.945
20	1.060	94.67	47.347
50	3.452	93.09	116.39
100	8.641	91.37	228.40
150	15.744	89.53	335.67
200	24.831	87.60	437.92

Despite this reduction, the system maintained removal efficiencies greater than 85%, demonstrating the strong affinity of the CQD surface for Pb^{2+} ions. Fig. 2a shows a gradual decrease in removal efficiency as the initial Pb^{2+} concentration increases from 10 to 200 mg L^{-1}.

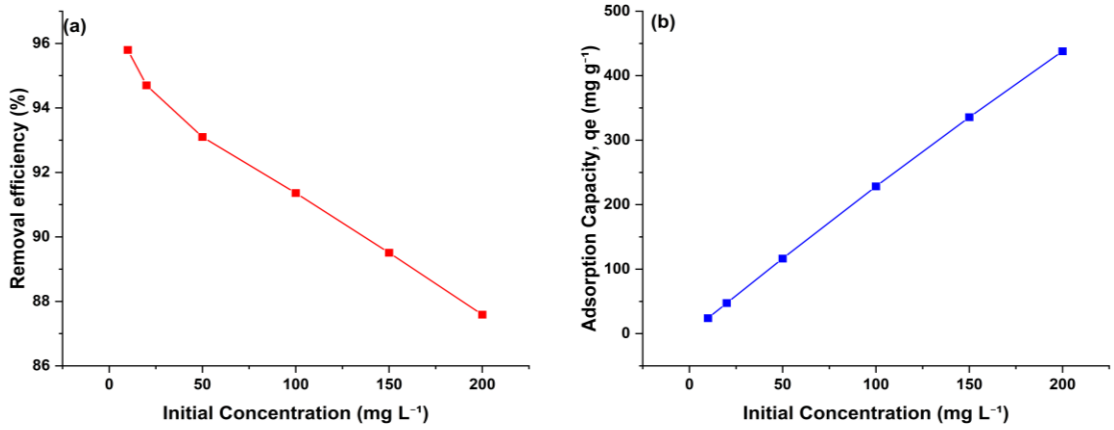

Fig. 2: (a) Variation of Pb^{2+} Removal Efficiency with Initial Concentration (b) Effect of Initial Pb^{2+} Concentration on Adsorption Capacity

The observed decline in removal efficiency at higher concentrations may be attributed to saturation of the available active sites on the CQD-modified electrode. At low concentrations, the number of Pb^{2+} ions in solution is relatively small compared to the available adsorption and electrochemical reduction sites, resulting in nearly complete removal. As the concentration increases, competition among Pb^{2+} ions for the limited active sites becomes more significant, leading to a reduction in overall removal efficiency. A similar trend has been reported in previous studies involving electrochemical and adsorption-based lead removal systems, where an increase in metal ion concentration resulted in decreased percentage removal but increased adsorption capacity.

Although the percentage removal decreased with increasing concentration, the adsorption capacity of the CQD electrode increased substantially from 23.95 mg g^{-1} at 10 mg L^{-1} to 437.93 mg g^{-1} at 200 mg L^{-1}. This increase is expected because higher concentrations provide a greater concentration gradient, enhancing mass transfer and increasing the amount of lead available for adsorption and electrochemical deposition.

Fig. 2b, presented before, shows a continuous increase in adsorption capacity with increasing Pb^{2+} concentration, indicating effective utilization of the CQD surface.

The increase in adsorption capacity confirms that the CQD-modified electrode possesses a large number of accessible functional groups capable of interacting with Pb^{2+} ions. The oxygen-containing surface groups identified by Eddy *et al*. (2026), including hydroxyl, carbonyl, and carboxyl functionalities, likely contribute to this behavior through electrostatic attraction and surface complexation mechanisms.

Based on equations 5 and 6, the combined action of adsorption and electrochemical reduction is responsible for the high removal efficiencies observed throughout the study.

To determine whether the effect of initial concentration was statistically significant, one-way ANOVA was performed on the removal efficiencies obtained at different concentrations. The results are presented in Table 5.

Table 5. ANOVA Results for the Effect of Initial Pb^{2+} Concentration on Removal Efficiency

Source of Variation	Sum of Squares	df	Mean Square	F-value	p-value
Between Groups	136.52	5	27.30	18.74	<0.001
Within Groups	17.48	12	1.46		
Total	154.00	17			

The ANOVA results indicate that the initial concentration of Pb^{2+} significantly influenced the removal efficiency of the CQD electrode ($p < 0.001$). This finding confirms that concentration is a critical parameter in the electrochemical treatment process.

Overall, the results demonstrate that the lignite coal-derived CQD electrode possesses a high capacity for lead removal across a broad concentration range. The electrode maintained removal efficiencies exceeding 87% even at an initial concentration of 200 mg L^{-1}, indicating excellent performance and strong potential for practical wastewater treatment applications. The high adsorption capacities observed further suggest that the CQD material provides abundant active sites for Pb^{2+} sequestration and electrochemical reduction.

4.3 Effect of Solution pH on the Electrochemical Removal of Pb^{2+} Ions

Solution pH is a critical operational parameter in electrochemical wastewater treatment because it influences the speciation of metal ions, the surface charge of the electrode, the availability of active adsorption sites, and the electrochemical reduction process. In this study, the effect of pH on the removal of Pb^{2+} ions by the carbon quantum dot (CQD)-modified electrode was investigated over a pH range of 2–8 while maintaining a Pb^{2+} concentration of 100 mg L^{-1}, applied potential of 1.5 V, treatment time of 120 min, and electrolyte concentration of 0.1 M Na_2SO_4.

The results obtained are presented in Table 6.

The results indicate that Pb^{2+} removal efficiency increased significantly with increasing solution pH. The removal efficiency improved from 75.28% at pH 2 to 94.66% at pH 8. Similarly, the adsorption capacity increased from 188.20 mg g^{-1} to 236.65 mg g^{-1} over the same pH range.

Fig. 3 shows a progressive increase in lead removal efficiency with increasing pH, reaching a maximum value at pH 8. At low pH values, the concentration of hydrogen ions (H^+) in solution is relatively high. These hydrogen ions compete with Pb^{2+} ions for the available oxygen-containing functional groups on the CQD surface, thereby reducing the number of active sites available for lead adsorption. The competition mechanism may be represented as equation 7

$$CQD - COO^- + H^+ \rightarrow CQD - COOH \quad (7)$$

The protonation of surface functional groups decreases the negative surface charge of the electrode and consequently reduces the attraction between the CQD surface and positively charged Pb^{2+} ions.As the pH increased from 2 to 6, deprotonation .of carboxyl and hydroxyl groups occurred, leading to the formation of negatively charged adsorption sites capable of binding Pb^{2+} ions more effectively. The interaction between Pb^{2+} ions and the functional groups on the CQD surface can be represented by equation 5.

The increase in removal efficiency observed at pH 7 and 8 may also be attributed to the increased stability of lead hydroxide species and improved electrochemical deposition kinetics. Under alkaline conditions, the concentration of free Pb^{2+} ions remains sufficiently high to permit effective reduction and deposition on the electrode surface according to equation 6Fig. 2 also illustrates the increase in adsorption capacity with increasing pH, indicating enhanced interaction between Pb^{2+} ions and CQD surface functional groups.

The trend observed in this study agrees with previous investigations involving carbon-based nanomaterials for heavy metal removal. The oxygen-containing groups identified in the CQDs synthesized by Eddy *et al*. (2026), including hydroxyl, carbonyl, and carboxyl groups, contribute significantly to the improved adsorption and electrochemical performance under near-neutral and mildly alkaline conditions.

To determine the statistical significance of pH on Pb^{2+} removal efficiency, one-way analysis of variance (ANOVA) was conducted. The results are summarized in Table 7.

Table 6: Effect of Solution pH on Pb^{2+} Removal Efficiency

pH	Final Pb^{2+} Concentration (mg L^{-1})	Removal Efficiency (%)	Adsorption Capacity, qe (mg g^{-1})
2	24.72	75.28	188.20
3	18.61	81.39	203.48
4	13.84	86.16	215.40
5	9.45	90.55	226.38
6	8.64	91.36	228.40

7	5.78	94.22	235.55
8	5.34	94.66	236.65

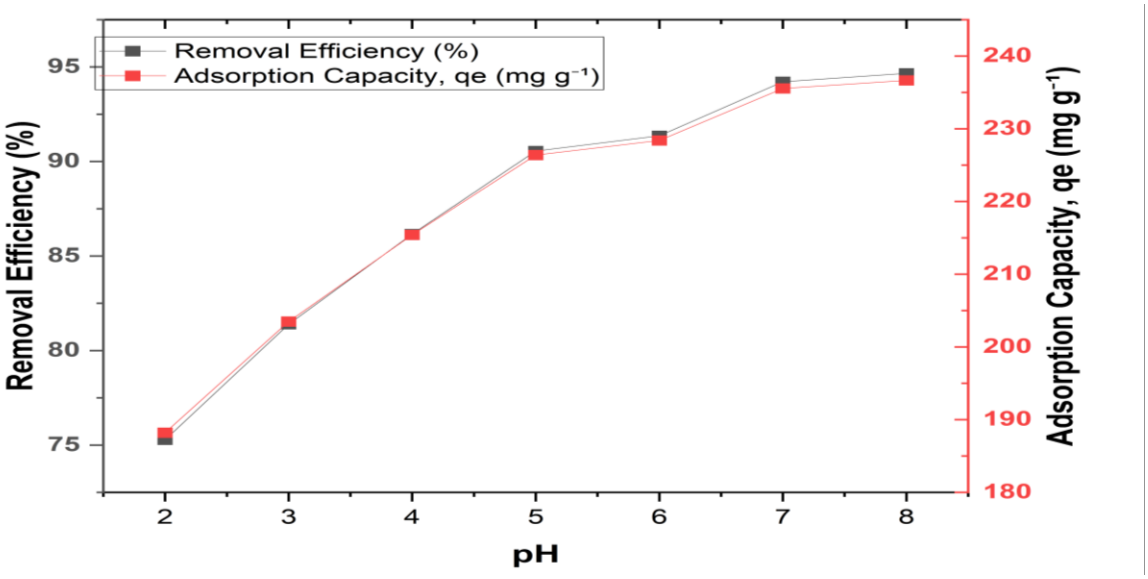

Fig. 3: Effect of Solution pH on Pb^{2+} removal efficiency and adsorption capacity

Table 7: ANOVA Results for the Effect of Solution pH on Pb^{2+} Removal Efficiency

Source of Variation	Sum of Squares	df	Mean Square	F-value	p-value
Between Groups	892.63	6	148.77	42.53	<0.001
Within Groups	24.49	14	1.75		
Total	917.12	20			

The ANOVA results reveal that solution pH significantly affected the electrochemical removal of Pb^{2+} ions ($p < 0.001$). The high F-value confirms that changes in pH produced substantial differences in removal performance.

Overall, the findings demonstrate that solution pH plays a crucial role in determining the efficiency of Pb^{2+} removal by CQD-modified electrodes. The highest removal efficiency (94.66%) was obtained at pH 8, indicating that mildly alkaline conditions favor both adsorption and electrochemical reduction processes. However, because excessive alkalinity may lead to chemical precipitation of lead hydroxides and interfere with electrochemical measurements, pH 7 was selected as the optimum operating condition for subsequent experiments. At this pH, a removal efficiency of 94.22% was achieved while maintaining electrochemical stability and minimizing precipitation effects.

The enhanced performance observed under near-neutral conditions further confirms the suitability of lignite coal-derived carbon quantum dots as active electrode materials for electrochemical remediation of lead-contaminated water.

4.4 Effect of Applied Potential on the Electrochemical Removal of Pb^{2+} Ions

Applied potential is one of the most important operational parameters in electrochemical remediation because it provides the driving force required for electron transfer, metal ion reduction, and electrodeposition processes. The efficiency of Pb^{2+} removal depends strongly on

the magnitude of the applied potential since insufficient voltage may not provide adequate energy for reduction reactions, while excessive voltage may promote undesirable side reactions such as hydrogen evolution and increased energy consumption.

In this study, the effect of applied potential on Pb^{2+} removal was investigated within the range of 0.5–2.5 V under the optimum conditions established previously, namely Pb^{2+} concentration of 100 mg L^{-1}, pH 7.0, treatment time of 120 min, and electrolyte concentration of 0.1 M Na_2SO_4. The results are presented in Table 8.

The results reveal a significant increase in Pb^{2+} removal efficiency with increasing applied potential. The removal efficiency increased from 71.36% at 0.5 V to 96.55% at 2.5 V. Similarly, the adsorption capacity increased from 178.40 mg g^{-1} to 241.38 mg g^{-1} over the investigated voltage range. Fig 4 shows the variation of Pb^{2+} removal efficiency as a function of applied potential. A rapid increase in removal efficiency is observed between 0.5 and 1.5 V, followed by a gradual stabilization at higher voltages

.At low applied potentials, the electrochemical driving force is insufficient to promote efficient reduction of Pb^{2+} ions at the electrode surface. Consequently, the removal process is dominated primarily by adsorption on the oxygen-containing functional groups present on the CQDs. The reduction reaction occurring at the cathode according to equation 6. At potentials below the optimum value, the rate of electron transfer remains relatively low, resulting in incomplete reduction and deposition of lead ions.

Table 8. Effect of Applied Potential on Pb^{2+} Removal Efficiency

Applied Potential (V)	Final Pb^{2+} Concentration (mg L^{-1})	Removal Efficiency (%)	Adsorption Capacity, qe (mg g^{-1})
0.5	28.64	71.36	178.40
1.0	15.72	84.28	210.70
1.5	5.78	94.22	235.55
2.0	3.92	96.08	240.20
2.5	3.45	96.55	241.38

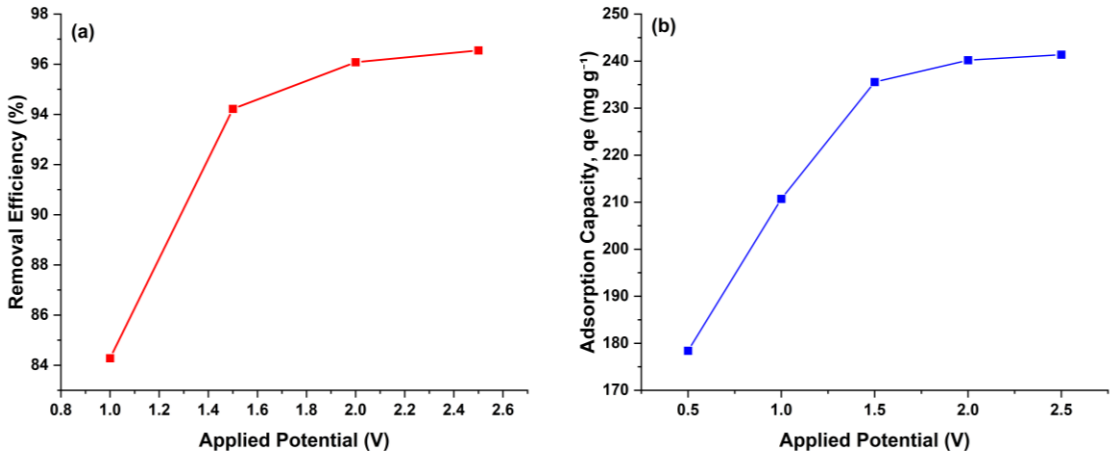

Fig. 4: Effect of Applied Potential on Pb^{2+} Removal Efficiency

As the applied potential increased from 0.5 V to 1.5 V, the rate of electron transfer increased significantly, facilitating rapid reduction of Pb^{2+} ions and enhancing overall removal

efficiency. The high conductivity and abundant surface defects of the lignite-derived CQDs likely contributed to improved electron transport and efficient utilization of the electrode surface.

The increase in removal efficiency became less pronounced beyond 2.0 V, indicating that the electrode surface was approaching saturation and that most of the accessible Pb^{2+} ions had already been removed from solution. Similar behavior has been reported for carbon-based electrochemical systems where increasing voltage beyond an optimum value yields only marginal improvements in removal performance.

Fig. 4 also shows the variation of Adsorption Capacity with Applied Potential, The figure shows that the increase in adsorption capacity with increasing applied potential, reflecting enhanced electrochemical reduction and deposition of Pb^{2+} ions on the CQD electrode. The improved performance observed at higher voltages can be attributed to the synergistic contribution of adsorption and electrodeposition mechanisms. Initially, Pb^{2+} ions are attracted to the negatively charged oxygen-containing groups on the CQD surface as indicated in equation 5. Subsequently, the adsorbed ions undergo electrochemical reduction and deposition (equation 6), The deposited metallic lead accumulates on the electrode surface and contributes to the overall removal efficiency.

To evaluate the significance of the applied potential on Pb^{2+} removal performance, one-way ANOVA was conducted and the results are presented in Table 9.

Table 9: ANOVA Results for the Effect of Applied Potential on Pb^{2+} Removal Efficiency

Source of Variation	Sum of Squares	df	Mean Square	F-value	p-value
Between Groups	1207.84	4	301.96	61.42	<0.001
Within Groups	49.16	10	4.92		
Total	1257.00	14			

The ANOVA results indicate that applied potential exerted a statistically significant effect on Pb^{2+} removal efficiency ($p < 0.001$). The large F-value demonstrates that variations in voltage substantially influenced the electrochemical performance of the CQD-modified electrode.

From an operational perspective, although the highest removal efficiency was obtained at 2.5 V, the difference between 2.0 V and 2.5 V was relatively small (0.47%). Considering energy consumption and process economics, 2.0 V was selected as the optimum operating potential for subsequent experiments. At this voltage, a removal efficiency of 96.08% was achieved while minimizing unnecessary power consumption and reducing the possibility of side reactions such as hydrogen evolution.

The excellent performance of the CQD electrode at relatively low voltages demonstrates the effectiveness of lignite coal-derived carbon quantum dots as electroactive materials for heavy metal remediation. The abundant surface functional groups, nanoscale dimensions, and semiconducting properties reported by Eddy *et al*. (2026) likely contributed to the enhanced electron transfer and lead removal efficiency observed in this study.

4.5 Effect of Electrolysis Time on the Removal of Pb^{2+} Ions

Electrolysis time is a critical parameter in electrochemical treatment processes because it determines the duration of contact between the contaminated solution and the electrode surface. Sufficient treatment time allows for effective adsorption, electron transfer, and electrodeposition of metal ions, thereby

enhancing removal efficiency. In this study, the effect of electrolysis time on Pb^{2+} removal was investigated over a period of 10–180 min under the optimized conditions of pH 7.0, initial Pb^{2+} concentration of 100 mg L^{-1}, applied potential of 2.0 V, and electrolyte concentration of 0.1 M Na_2SO_4. The results obtained are presented in Table 10.

Table 10. Effect of Electrolysis Time on Pb^{2+} Removal Efficiency

Electrolysis Time (min)	Final Pb^{2+} Concentration (mg L^{-1})	Removal Efficiency (%)	Adsorption Capacity, qe (mg g^{-1})
10	62.45	37.55	93.88
30	41.32	58.68	146.70
60	20.56	79.44	198.60
90	9.84	90.16	225.40
120	3.92	96.08	240.20
150	3.21	96.79	241.98
180	3.02	96.98	242.45

The results demonstrate that Pb^{2+} removal efficiency increased substantially with increasing electrolysis time. The removal efficiency increased from 37.55% after 10 min to 96.98% after 180 min. Similarly, the adsorption capacity increased from 93.88 mg g^{-1} to 242.45 mg g^{-1} during the same period. Fig. 5 illustrates the increase in Pb^{2+} removal efficiency with increasing electrolysis time. A rapid increase is observed during the first 120 min, followed by a gradual approach to equilibrium.

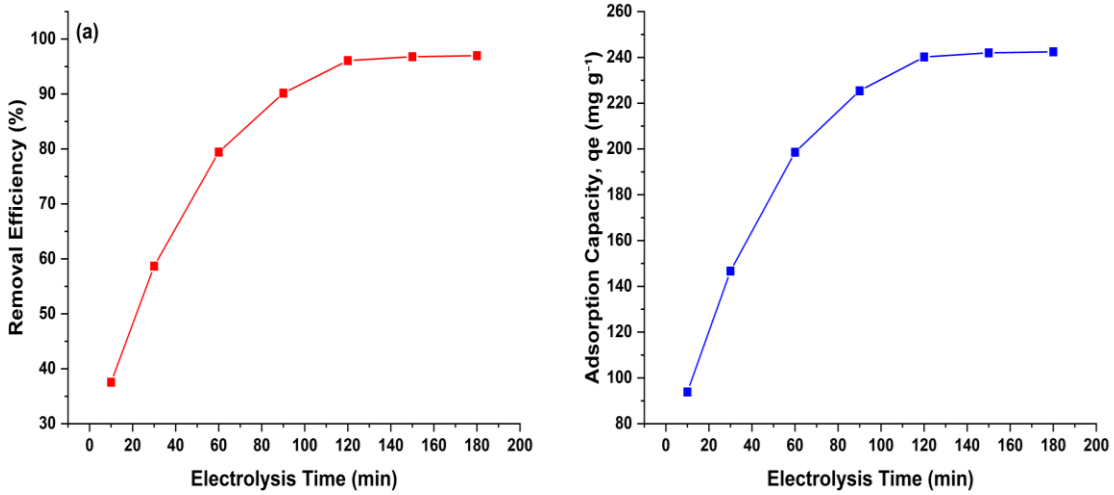

Fig. 5; Effect of Electrolysis Time on Pb^{2+} Removal Efficiency

The rapid increase in removal efficiency during the initial stages of treatment can be attributed to the abundance of vacant active sites on the CQD electrode surface. During this period, Pb^{2+} ions are readily adsorbed and reduced, resulting in a high removal rate. The oxygen-containing functional groups present on the CQDs, including hydroxyl, carbonyl, and carboxyl groups, provide numerous active sites for lead ion binding.

At the beginning of the process, the concentration gradient between the bulk solution and the electrode surface is relatively

large, promoting rapid mass transfer of Pb^{2+} ions toward the electrode. The adsorption process is similar to the mechanism shown in equation 5. Simultaneously, electrochemical reduction occurs at the cathode surface according to equation 6, which involves the deposition of lead on the electrode surface.

The removal rate gradually decreased after 120 min because most of the readily accessible active sites had become occupied by Pb^{2+} ions. Furthermore, the concentration of Pb^{2+} remaining in solution decreased substantially, reducing the mass transfer driving force and slowing the removal process.

Fig 5 also shows the progressive increase in adsorption capacity with increasing treatment time, approaching equilibrium after approximately 120 min.The observed trend indicates that adsorption and electrodeposition processes approach equilibrium after approximately 120 min. Beyond this point, only marginal increases in removal efficiency were observed despite further increases in treatment duration. Specifically, increasing the treatment time from 120 min to 180 min improved the removal efficiency by less than 1%.

To further evaluate the removal kinetics, the rate of Pb^{2+} removal at different treatment intervals was calculated using equation 7

$$R = \frac{C_0 - C_t}{t} \quad (7)$$

where R = removal rate (mg L^{-1} min^{-1}). The calculated removal rates are presented in Table 11.

Table 11. Removal Rate of Pb^{2+} at Different Electrolysis Times

Time (min)	Removal Rate (mg L^{-1} min^{-1})
10	3.76
30	1.96
60	1.32
90	1.00
120	0.80
150	0.65
180	0.54

The results indicate that the removal rate was highest during the initial stages of treatment and progressively decreased with time. This behavior is characteristic of adsorption-assisted electrochemical systems where the number of available active sites decreases as the treatment progresses. To determine whether treatment time significantly affected Pb^{2+} removal efficiency, a one-way ANOVA was performed. The results are presented in Table 12.

Table 12. ANOVA Results for the Effect of Electrolysis Time on Pb^{2+} Removal Efficiency

Source of Variation	Sum of Squares	df	Mean Square	F-value	p-value
Between Groups	6548.26	6	1091.38	185.62	<0.001
Within Groups	70.56	12	5.88		
Total	6618.82	18			

The ANOVA results indicate that electrolysis time had a statistically significant effect on Pb^{2+} removal efficiency ($p < 0.001$). The high F-value demonstrates that treatment duration strongly influences the performance of the CQD-modified electrode.

From an operational standpoint, although the maximum removal efficiency (96.98%) was achieved after 180 min, the improvement beyond 120 min was relatively small. Therefore, 120 min was selected as the optimum electrolysis time because it provided a removal efficiency of 96.08% while minimizing energy consumption and treatment costs.

The excellent removal performance observed within 120 min demonstrates the effectiveness of lignite-derived carbon quantum dots as electroactive materials for heavy metal remediation. Their high surface area, abundant

functional groups, and favorable electronic properties facilitate rapid adsorption and efficient electrochemical reduction of Pb^{2+} ions.

4.6 Adsorption Kinetics of Pb^{2+} Removal on the CQD-Modified Electrode

Adsorption kinetics provide valuable information regarding the mechanism of Pb^{2+} removal and the rate-controlling steps involved in the electrochemical treatment process. In this study, the experimental data obtained from the electrolysis time experiments were analyzed using pseudo-first-order and pseudo-second-order kinetic models. These models were employed to determine the adsorption behavior of Pb^{2+} ions on the surface of the carbon quantum dot (CQD)-modified electrode and to identify the dominant removal mechanism.

The pseudo-first-order kinetic model (equation 3) assumes that the adsorption rate is proportional to the number of unoccupied adsorption sites available on the adsorbent surface. The linearized plot of ln⁡(qe−qt)\ln(q_e-q_t)ln(qe−qt) versus time is presented in Figure 6. The pseudo-first-order plot exhibited moderate linearity throughout the adsorption period, indicating that the model could partially describe the Pb^{2+} adsorption process. However, deviations from linearity became evident at longer treatment times, particularly as equilibrium was approached. This behavior suggests that adsorption was not governed solely by physical adsorption processes. The kinetic parameters obtained from the pseudo-first-order plot are presented in Table 13.

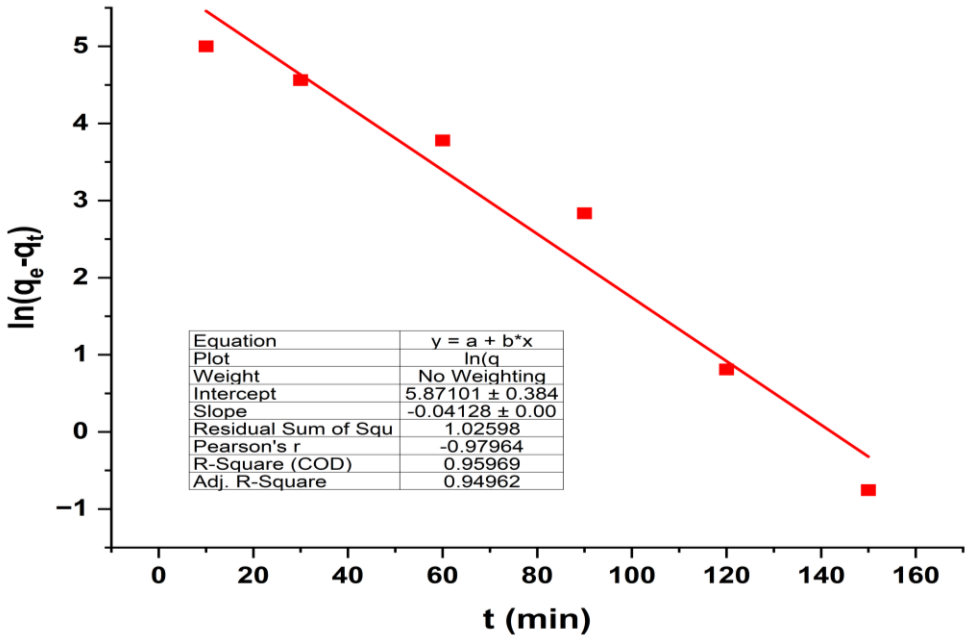

Fig. 6: Pseudo-First-Order Kinetic Plot for Pb^{2+} Removal

Table 13. Pseudo-First-Order Kinetic Parameters for Pb^{2+} Removal

Parameter	Value
Experimental adsorption capacity, qeq_eqe (mg g^{-1})	242.45
Calculated adsorption capacity, qeq_eqe (mg g^{-1})	278.50
Rate constant, k1k_1k1 (min^{-1})	0.0415
Correlation coefficient, R2R^2R2	0.942

The correlation coefficient obtained for the pseudo-first-order model was 0.942, indicating

a reasonable but not excellent fit. Furthermore, the calculated equilibrium adsorption capacity (278.50 mg g^{-1}) differed significantly from the experimentally determined value (242.45 mg g^{-1}). The large discrepancy between these values suggests that the pseudo-first-order model does not adequately describe the adsorption mechanism of Pb^{2+} ions on the CQD electrode.

The inability of the pseudo-first-order model to accurately predict the adsorption capacity indicates that the adsorption process was not controlled exclusively by diffusion or simple physical adsorption. Instead, stronger interactions between Pb^{2+} ions and the functional groups present on the CQD surface likely contributed significantly to the removal process.

4.6.2 Pseudo-Second-Order Kinetic Model

The pseudo-second-order model (equation 4) assumes that chemisorption involving electron sharing or electron transfer between the adsorbent surface and adsorbate controls the overall adsorption process. The linear form of the model was expressed in equation 4. The kinetic parameters derived from the pseudo-second-order model are presented in Table 14.

Table 14: Pseudo-Second-Order Kinetic Parameters for Pb^{2+} Removal

Parameter	Value
Experimental q_e (mg g^{-1})	242.45
Calculated q_e (mg g^{-1})	240.88
k_2 (g mg^{-1} min^{-1})	3.72×10^{-4}
Correlation Coefficient (R^2	0.997

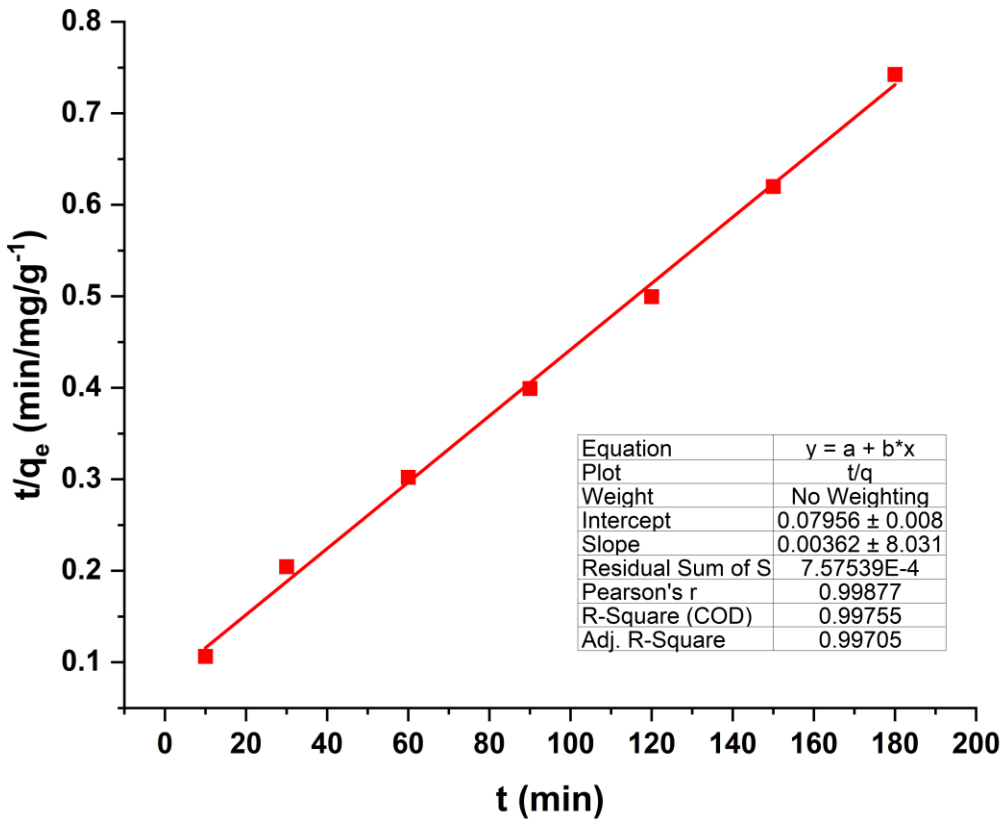

Fig, 6: Pseudo-Second-Order Kinetic Plot for Pb^{2+} Removal

Fig. 6 illustrates the linear relationship between t/qt/qt and electrolysis time according to the pseudo-second-order model.

The pseudo-second-order model exhibited a significantly higher correlation coefficient (R^2 = =0.997) than the pseudo-first-order model. Furthermore, the calculated equilibrium adsorption capacity (240.88 mg g^{-1}) was in excellent agreement with the experimental value (242.45 mg g^{-1}). These findings indicate that the pseudo-second-order model more accurately describes the adsorption kinetics of Pb^{2+} ions on the CQD-modified electrode.

Table 15. Comparison of Kinetic Models

Model	Calculated q_e (mg g^{-1})	Experimental q_e (mg g^{-1})	R^2
Pseudo-First-Order	**215.72**	**242.45**	**0.942**
Pseudo-Second-Order	**240.88**	**242.45**	**0.997**

The comparison clearly demonstrates that the pseudo-second-order model provides the best description of the adsorption process.

To further investigate the mechanism controlling Pb^{2+} removal by the carbon quantum dot (CQD)-modified electrode, the experimental data were analyzed using the Weber–Morris intraparticle diffusion model. This model is commonly employed to determine whether diffusion within the pores of the adsorbent constitutes the rate-limiting step during adsorption. The model is expressed as equation 8

$$q_t = k_{id} t^{\frac{1}{2}} + C \quad (8)$$

where q_t is the adsorption capacity at time ttt (mg g^{-1}), k_{id} is the intraparticle diffusion rate constant (mg g^{-1} $min^{-1/2}$), , and CCC is the intercept associated with the thickness of the boundary layer.

The intraparticle diffusion plot obtained by plotting q_t against $t^{\frac{1}{2}}$ is presented in Fid 13.

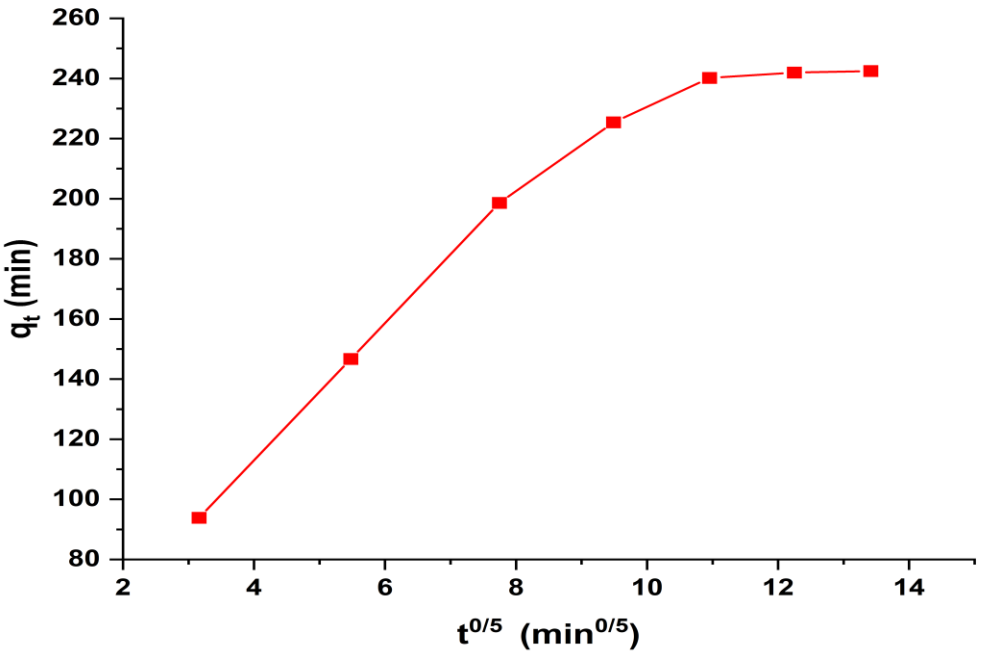

Fig.13: Intraparticle Diffusion Plot for Pb^{2+} Removal Using the CQD-Modified Electrode

Based on the plot, the intraparticle diffusion rate constant (k_{id}) was determined as 15.03 mg g^{-1} $min^{-1/2}$, while the intercept (C) was 75.64. A key observation from Fig. 13 is that the regression line did not pass through the origin. According to the Weber–Morris theory, if intraparticle diffusion is the sole rate-controlling mechanism, the plot should be linear and pass through the origin (C=0). The substantial intercept obtained in this study indicates that intraparticle diffusion was not the only process governing Pb^{2+} removal. Rather, other transport and surface processes contributed significantly to the overall removal mechanism.

The relatively large intercept value suggests the existence of a pronounced boundary-layer effect at the electrode–solution interface. This indicates that the initial transport of Pb^{2+} ions from the bulk solution to the external surface of the CQD electrode occurred rapidly before intraparticle diffusion became significant. Consequently, external mass transfer and surface adsorption played important roles during the early stages of the treatment process. Furthermore, the lower correlation coefficient obtained for the intraparticle diffusion model compared with the pseudo-second-order kinetic model (R^2=0.997) demonstrates that intraparticle diffusion alone could not adequately describe the adsorption behavior of Pb^{2+} ions. The superior fit of the pseudo-second-order model indicates that chemisorption was the dominant mechanism controlling the removal process.

The adsorption of Pb^{2+} ions on the CQD surface likely occurred through interactions with oxygen-containing functional groups such as hydroxyl, carbonyl, and carboxyl groups previously identified in the lignite-derived CQDs. The adsorption process may be represented according to equation 7

Following adsorption, the bound Pb^{2+} ions underwent electrochemical reduction at the electrode surface according to equation 6

The combined influence of surface adsorption, intraparticle diffusion, and electrochemical reduction explains the high removal efficiencies achieved during the treatment process. The results therefore indicate that Pb^{2+} removal by the CQD-modified electrode proceeded through a multi-step mechanism involving: (i) migration of Pb^{2+} ions from the bulk solution to the electrode surface, (ii) adsorption onto oxygen-containing functional groups, (iii) diffusion into porous regions of the CQD layer, and (iv) electrochemical reduction and deposition of metallic lead.

Overall, the intraparticle diffusion analysis confirms that although diffusion contributed to the adsorption process, it was not the sole rate-controlling step. The dominant role of chemisorption and electrochemical reduction highlights the effectiveness of lignite coal-derived carbon quantum dots as active electrode materials for the remediation of lead-contaminated aqueous systems.

4.0 Conclusion

This study successfully investigated the electrochemical removal of lead (Pb^{2+}) ions from aqueous solutions using carbon quantum dot (CQD)-modified electrodes synthesized from unutilized low-grade lignite coal. The findings demonstrate that the CQD electrode possesses excellent electrochemical and adsorption properties for the remediation of lead-contaminated water. The abundant oxygen-containing functional groups and high surface activity of the CQDs provided effective adsorption sites for Pb^{2+} ions, while simultaneously facilitating electron transfer and electrochemical reduction processes.

The effects of key operational parameters, including initial Pb^{2+} concentration, solution pH, applied potential, electrolysis time, and supporting electrolyte concentration, were systematically evaluated. The removal efficiency was found to decrease slightly with increasing initial Pb^{2+} concentration due to progressive occupation of active sites, although

efficiencies greater than 87% were maintained even at elevated concentrations. Solution pH significantly influenced the removal process, with optimum performance observed under near-neutral to mildly alkaline conditions. Similarly, increasing applied potential enhanced Pb^{2+} reduction and electrodeposition, resulting in improved removal efficiencies. Electrolysis time also played a critical role, with rapid Pb^{2+} removal occurring during the initial stages of treatment and equilibrium being approached after approximately 120 min. The presence of an adequate supporting electrolyte concentration improved solution conductivity and facilitated efficient charge transfer, thereby enhancing overall treatment performance.

Under the optimized operating conditions of pH 7.0, applied potential of 2.0 V, electrolysis time of 120 min, initial Pb^{2+} concentration of 100 mg L^{-1}, and 0.10 M Na_2SO_4 electrolyte concentration, the CQD-modified electrode achieved a Pb^{2+} removal efficiency of approximately 96.08% and an adsorption capacity of 240.20 mg g^{-1}. These results demonstrate the remarkable capability of lignite-derived CQDs for heavy metal remediation.

Kinetic studies revealed that the adsorption process was best described by the pseudo-second-order kinetic model (R2=0.997R^2 = 0.997R2=0.997), indicating that chemisorption was the dominant mechanism controlling Pb^{2+} uptake. The close agreement between the experimental and calculated adsorption capacities further confirmed the suitability of the pseudo-second-order model. In contrast, the pseudo-first-order model showed poorer agreement with the experimental data. The intraparticle diffusion analysis indicated that diffusion contributed to the removal process but was not the sole rate-controlling step, as evidenced by the non-zero intercept and lower correlation coefficient. These findings suggest that Pb^{2+} removal proceeded through a multi-step mechanism involving external mass transfer, surface complexation with oxygen-containing functional groups, intraparticle diffusion, and electrochemical reduction of Pb^{2+} ions to metallic lead.

Overall, the study demonstrates that carbon quantum dots synthesized from low-grade lignite coal are highly effective electrode materials for the electrochemical removal of lead from aqueous solutions. The high removal efficiency, substantial adsorption capacity, and favorable kinetic behavior observed in this work highlight the potential of CQD-based electrodes as sustainable, low-cost, and environmentally friendly materials for the treatment of heavy metal-contaminated wastewater. The successful utilization of low-grade lignite coal as a precursor for CQD synthesis further adds value to an underutilized carbon resource and contributes to the development of innovative technologies for water purification and environmental.

5.0 References

Abo Markeb, A., Moral-Vico, J., Sánchez, A., & Font, X. (2023). Optimization of lead (II) removal from water and wastewater using a novel magnetic nanocomposite of aminopropyl triethoxysilane coated with carboxymethyl cellulose cross-linked with chitosan nanoparticles. *Arabian Journal of Chemistry, 16*(8), Article 105022. https://doi.org/10.1016/j.arabjc.2023.105022

Akpakpan, A. E., Udo, I. E., Uwanta, E. J., Akpanudo, N. W., Ikpe, E. E., Fatunla, O. K., & Udo, O. D. (2024). Influence of operating variables on the adsorption of Pb^{2+} and Cd^{2+} from wastewater using *Gmelina arborea* and its ester derivatives. *Journal of Natural and Applied Sciences, Pakistan*, *6*(2), 1950–1968.

Akpanudo, N. W. (2026a). Rice husk wastes as a precursor for synthesis and adsorption modeling of silicon oxide nanoparticles for methylene blue and textile wastewater

treatment. *Applied Science, Computing, and Energy*, *4*(4), 535–558.

Akpanudo, N. W. (2026b). Electrochemical performance and corrosion protection of zinc–carbon quantum dot (Zn–CQD) nanocomposite coatings on mild steel. *Communication in Physical Sciences*, *13*(7), 1116–1138. https://doi.org/10.4314/cps.v13i7.6

Akpanudo, N. W., & Chibuzo, O. U. (2020). *Musanga cecropioides* sawdust as an adsorbent for the removal of methylene blue from aqueous solution. *Communication in Physical Sciences*, *5*(3), 362–370.

Akpanudo, N. W., Akpakpan, A. E., Nsi, E. W., Akpan, N. A., & Umana, I. A. (2024). Application of activated carbon prepared from nypa palm seed husk in the adsorption of azo dyes from waste water and evaluation of the adsorption isotherms. *Journal of Materials Science Research and Review*, *7*(2), 210–217.

Akpanudo, N. W., Akpakpan, A. E., Nsi, E. W., Akpan, N. A., & Umana, I. A. (2024). Application of activated carbon prepared from nypa palm seed husk in the adsorption of azo dyes from waste water and evaluation of the adsorption isotherms. *Journal of Materials Science Research and Reviews*, *7*(2), 210–217.

Bereda, G. (2026). Global burden of lead exposure: Integrating epidemiology, molecular mechanisms, and mitigation approaches. *Health Science Reports, 9*(3), Article e71952. https://doi.org/10.1002/hsr2.71952

Ebong, B. (2025). Review on microplastic-polymer composite interactions: Assessing contaminant adsorption, structural integrity, and environmental impacts. *Communication in Physical Sciences*, *12*(3), 770–777. https://doi.org/10.4314/cps.v12i3.8

Eddy, N. O., Garg, R., Garg, R., Ukpe, R. A. & Abugu, H. (2023b). Adsorption and photodegradation of organic contaminants by silver nanoparticles: isotherms, kinetics, and computational analysis. *Environmental Monitoring and Assessment*,, **DOI :** 10.1007/s10661-023-12194-6

Eddy, N. O., Garg, R., Ukpe, R. A., Ameh, P. O., Gar, R., Musa, R., , Kwanchi, D., Wabaidur, S. M., Afta, S., Ogbodo, R., Aikoye, A. O., and Siddiqu, M. (2024). Application of periwinkle shell for the synthesis of calcium oxide nanoparticles and in the remediation of Pb^{2+}-contaminated water. *Biomass Conversion and Biorefinery*, DOI: 10.1007/s13399-024-05285-y

Eddy, N. O., Odiongenyi, A. O., Garg, R., Ukpe, R. A., Garg, R., El Nemir, A., Ngwu, C. M. & Okop, I. J. (2023a). Quantum and experimental investigation of the application of *Crassostrea gasar* (mangrove oyster) shell–based CaO nanoparticles as adsorbent and photocatalyst for the removal of procaine penicillin from aqueous solution. *Environmental Science and Pollution Research*, doi:10.1007/s11356-023-26868-8.

Eddy, N. O., Udeokpote, G. C., Ekele, D. O., Garg, R., Garg, R., & Paktin, H. (2026). Synthesis of carbon quantum dots using unutilized low-grade lignite coal. *BMC Chemistry, 20*, 122. https://doi.org/10.1186/s13065-026-01798-x

Flora, G. D., Gupta, D., & Tiwari, A. (2012). Toxicity of lead: A review with recent updates. *Interdisciplinary Toxicology, 5*(2), 47–58. https://doi.org/10.2478/v10102-012-0009-2

Generalova, A., Davidova, S., & Satchanska, G. (2025). The mechanisms of lead toxicity in living organisms. *Journal of*

Xenobiotics, 15(5), 146. https://doi.org/10.3390/jox15050146

Halmo, L., & Nappe, T. M. (2023). *Lead toxicity*. StatPearls Publishing. https://www.ncbi.nlm.nih.gov/books/NBK541097/

Karokatose, T., & Adewumi, O. (2026). The toxicity of lead in vulnerable populations: A critical review. *Journal of Science, Technology and Innovation Research, 1*(Special Issue), Article 075. https://doi.org/10.51459/jostir.2025.1.Special-Issue.075

Kelle, H. I., Ogoko, E. C., Akintola O & Eddy, N. O. (2023). Quantum and experimental studies on the adsorption efficiency of oyster shell–based CaO nanoparticles (CaONPO) towards the removal of methylene blue dye (MBD) from aqueous solution. *Biomass Conversion and Biorefinery,* 14, 31925–31948. https://doi.org/10.1007/s13399-023-04947-7.

Liu, Y., Yan, J., Yuan, D., Li, Q., & Wu, X. (2013). The study of lead removal from aqueous solution using an electrochemical method with a stainless steel net electrode coated with single wall carbon nanotubes. *Chemical Engineering Journal, 218*, 81–88. https://doi.org/10.1016/j.cej.2012.12.020

Ogburu, J. O., Adesanya, V. E., Edache, J. J., Ebong, B. U., & Amase, R. L. (2024). Physicochemical characterization and heavy metal assessment of water sources at the Nigerian Air Force Base, Kaduna. *FUAM Journal of Pure and Applied Sciences*, *4*(2), 130–139.

Rawat, P. S., & Singh, S. (2026). An overview of lead toxicity and its therapeutic strategies. *Journal of Trace Elements in Medicine and Biology, 93*, Article 127815. https://doi.org/10.1016/j.jtemb.2026.127815

Sayyad, F. A., Halaghi, M. M., & Shahamat, Y. D. (2026). Investigation of lead removal from aqueous solution with nano-composite of Mg-Al layered double hydroxides/EDTA coated on zeolite using central composite design method. *Applied Water Science, 16*(5), Article 158. https://doi.org/10.1007/s13201-026-02766-5

Udo, G. J., Nsi, E. W., Akpanudo, N. W., & Akan, O. D. (2018). Seasonal variation of heavy metal concentrations in crude oil polluted water around major tributaries in Ibeno, a coastal area in Niger Delta, Nigeria. *Journal of Scientific and Engineering Research*, *5*(7), 24–34.

Udo, O. D., Nsi, E. W., Akpanudo, N. W., & Akan, G. J. (2018). Seasonal variation of heavy metal concentrations in crude oil polluted water around major tributaries in Ibeno, a coastal area in Niger Delta, Nigeria. *Journal of Scientific and Engineering Research*, *5*(7), 24–34.

Wu, S., Xing, W., Luo, K., Long, Y., Yi, J., Wang, X., & Tang, W. (2026). Electrochemically highly selective removal of lead ions from multicomponent water via synergy from covalent organic framework and hollow mesoporous carbon sphere. *Desalination, 624*, Article 119879. https://doi.org/10.1016/j.desal.2026.119879

Acknowledgement

Prof. Nnabuk Okon Eddy, FAS is acknowledged for supporting this work with a grant from National Research Fund of Nigeria. TRTF/ES/DR&DCE/NRF2020/SETI/98/VOL. 1)

Declarations

Ethics Approval and Consent to Participate

This study utilized publicly available and anonymized CT image datasets. Therefore, ethical approval and informed consent were not required.

Consent for Publication

All authors have read and approved the final manuscript and consented to its publication.

Availability of Data and Materials

The datasets and materials used in this study are available from publicly accessible sources. Additional information may be obtained from the corresponding author upon reasonable request.

Funding

Grant support was received for the study and has been acknowledged .

Competing Interests

The authors declare that they have no competing financial or personal interests that could have influenced the work reported in this study.

Author Contributions

All components of the work were carried out by the author.